

Raman scattering and the evolution of polar order in Li-doped and Nb-doped KTaO_3

P. Calvi, P. Camagni, E. Giolotto, and L. Rollandi

Dipartimento di Fisica "Alessandro Volta," Via Bassi 6, 27100 Pavia, Italy

(Received 8 December 1994; revised manuscript received 8 June 1995)

A comparative study of first-order Raman scattering in $\text{K}_{0.984}\text{Li}_{0.016}\text{TaO}_3$ and $\text{KTa}_{0.976}\text{Nb}_{0.024}\text{O}_3$ single crystals has been performed. The soft-phonon line shows marked differences in the two systems, revealing a distinctive behavior with regard to the scale of polar order. Analysis of the low-frequency spectrum allows for an estimate of the polar correlation length in the Li-doped sample; this is limited to the nanometric scale, in agreement with the view of a dipole-glass transition. No evidence of a similar situation is found in the Nb-doped sample, where the general trend of soft-mode frequencies and intensities suggests a transition to a state of long-range order, for the quoted concentration. The intensities of the hard-phonon spectra and the TO_4 linewidth are shown to confirm the different evolution of the polar transition in the two systems.

I. INTRODUCTION

KTaO_3 is an oxidic perovskite with an incipient ferroelectric behavior. The system remains centrosymmetric at all temperatures, but shows a divergent dielectric susceptibility due to the softening of the TO_1 transverse-optic mode as $T \rightarrow 0$ K. This mode involves atomic displacements along Ta-O chains.

The presence of substitutional impurities such as Nb or Li is known to induce a transition to a polar phase at finite temperatures, whose nature depends on the type and concentration of the specific impurity.¹⁻³ In $\text{KTa}_{1-x}\text{Nb}_x\text{O}_3$ (KTN) the substitution of Nb for Ta promotes directly the dynamical instability of the ferroelectric chain;⁴ this view is supported by a number of observations according to which one or more structural phase transitions occur in this system above a concentration $x=0.008$.⁵⁻⁷ At the same time, Nb ions possess a fast hopping motion between off-center minima along $\langle 111 \rangle$ directions, which is also revealed by the presence of order-disorder features in the vicinity of the transition.^{8,9} The progressive freezing of these motions is connected to the formation of clusters, whose role in the polar phase is controversial.^{10,11} In dilute systems, configurational disorder is claimed to prevail, giving rise to a glassy state.^{9,12,13}

Light scattering is of special utility in investigating these problems, as it probes symmetry breaking and dynamical aspects at the same time. In KTN a good deal of work has been devoted to investigate the behavior of the soft mode and the effects of local Nb dynamics. Although the low-frequency spectra of KTN, with $x \geq 1.2\%$, are usually interpreted in terms of a displacive transition, incomplete softening of the TO_1 mode and the behavior of central-peak features in dilute samples have been taken as indications of dipole-glass properties.¹⁴⁻¹⁶ Further emphasis on clustering phenomena is brought by recent studies of hard-phonon modes.^{17,18}

The role played by Li in $\text{K}_{1-x}\text{Li}_x\text{TaO}_3$ (KLT) is quite different. It substitutes for K and can jump between six equivalent minima along pseudocubic directions; the large off-center displacement^{19,20} and ionic radius misfit give rise to strong dipolar and elastic moments. Consequently descriptions are based on the random coupling of Li dipoles, leading

to a disordered polar state at low doping.^{1,21} In recent work a nonlinear shell model was applied to the calculation of the Li-Li interaction energy;²² this was found to be strongly dependent on relative dipole orientation as well as on bond distance and direction. Correspondingly, ferroelectric order should be frustrated. The view of a glassy state is supported by a variety of experiments such as dielectric relaxation,²³ second-harmonic generation,²⁴ ultra-acoustic attenuation,²⁵ and microwave mixing.²⁶ In contrast with the accepted picture, early analysis of Raman spectra seemed to support the idea of a ferroelectric transition.²⁷ More recent results have shown that the intense first-order spectra observed at low concentration are related to the presence of polar microregions rather than to long-range order.²⁸

In the authors' opinion, the existing Raman work leaves some space for further investigation in KTN and KLT, aiming to a comparative survey as regards the evolution and the final structure of polar order. This is particularly needed in systems at low concentration. Past Raman studies have shown the utility of line-shape analysis, with special regard to the soft-mode spectrum, which is a sensitive probe of polar correlation.^{29,30} In this view, the present work develops a detailed study of two representative systems by combining spectral analysis and line strength observations of both soft- and hard-phonon spectra.

II. EXPERIMENT

The present experiments refer to samples of $\text{KTa}_{0.976}\text{Nb}_{0.024}\text{O}_3$ (KTN) and $\text{K}_{0.984}\text{Li}_{0.016}\text{TaO}_3$ (KLT), grown by the spontaneous nucleation technique. The KTN sample was cut along the planes (111), $(1\bar{1}0)$, $(11\bar{2})$ of the cubic phase. The KLT sample was cut along the pseudocubic faces. The electroded faces were (111) and (001), respectively.

The transition temperatures, marking the onset of the polar phase in the two systems, can be accurately defined by the sharp increase of birefringence.^{11,31} By this method we actually characterized a critical temperature $T_c=32$ K for KTN and a freezing temperature $T_f=36.5$ K for KLT. By monitoring the birefringence in successive cooling and heating cycle,

the absence of thermal hysteresis in both systems was confirmed.

Raman measurements were taken with a Ramanor spectrometer (Jobin & Yvon Mod. HG-2S). Excitation was provided by the 514 nm line of an Ar-ion laser (Coherent INNOVA 300). The samples were mounted in a helium closed-cycle optical cryostat (Leybold Mod. R 210) under control of a Lakeshore Mod. 330 temperature controller. The experiments were performed cooling the samples in zero field (ZFC) or in the presence of a poling field of 2 kV/cm along the z direction (FC). Cooling between successive measurements was effected at a rate of 1 K/min. Spectral resolution was set at 1 cm^{-1} for KTN and 2 cm^{-1} for KLT. First-order spectra from transverse-optic modes were recorded over the range from 100 to 15 K. The scattered intensities from the two samples were normalized with respect to the second-order spectra at room temperature, which are insensitive to doping. The spectra discussed in this paper were obtained in $x(zz)y$ geometry.

In monitoring Raman spectra in a poled crystal one is aware of possible artifacts, due to carrier injection by a relatively intense exciting light. The drift of these carriers can easily produce space-charge effects which partly counteract the external field, thus depressing the evolution of poling. This possibility can be ruled out for KTN, on the ground that our sample did not show excess conduction with respect to dark-current levels ($<10^{-10} \text{ A}$) when irradiated with a 100 mW laser beam, in fields up to 1000 V/cm. The absence of photocurrents in this material, at low Nb concentrations, has already been noticed by other authors.³²

In similar conditions, sizeable photocurrents were found to take place in our KLT below T_f , again in agreement with earlier observations.³² In conjunction with this we noticed the presence of space-charge effects which make measurements less reliable at intermediate temperatures where polar relaxation is possible. Below 20 K, however, polarization is completely frozen and the Raman probe is nonintrusive, inasmuch as the sample be poled *in the dark* to these temperatures before observation.

III. RESULTS AND DISCUSSION

A. Soft-phonon spectrum

KTN. Figure 1(a) shows the spontaneous (ZFC) evolution of the low-frequency Raman spectrum, both Stokes and anti-Stokes, in a temperature range covering the transition. In the immediate vicinity of T_c one notices the simultaneous growth of a broad central component C and of the soft-phonon line: these are usually interpreted as scattering from a relaxational mode, coupled to the TO_1 soft mode¹⁴ whose appearance above $\sim T_c$ reflects precursor order.³³ On further cooling, the C line narrows and weakens; the TO_1 line emerges from the background, growing in intensity and frequency and splitting in two components. At the lowest T 's, both the strength and the shape of this line are largely independent of poling conditions: this is shown in Fig. 1(b), comparing the final spectra obtained at 17 K in zero-field and field-cooling conditions.

We have attempted to analyze the spectral shape, in the spontaneous case, distinguishing the following: (i) a temperature range around T_c , where the coupling between relax-

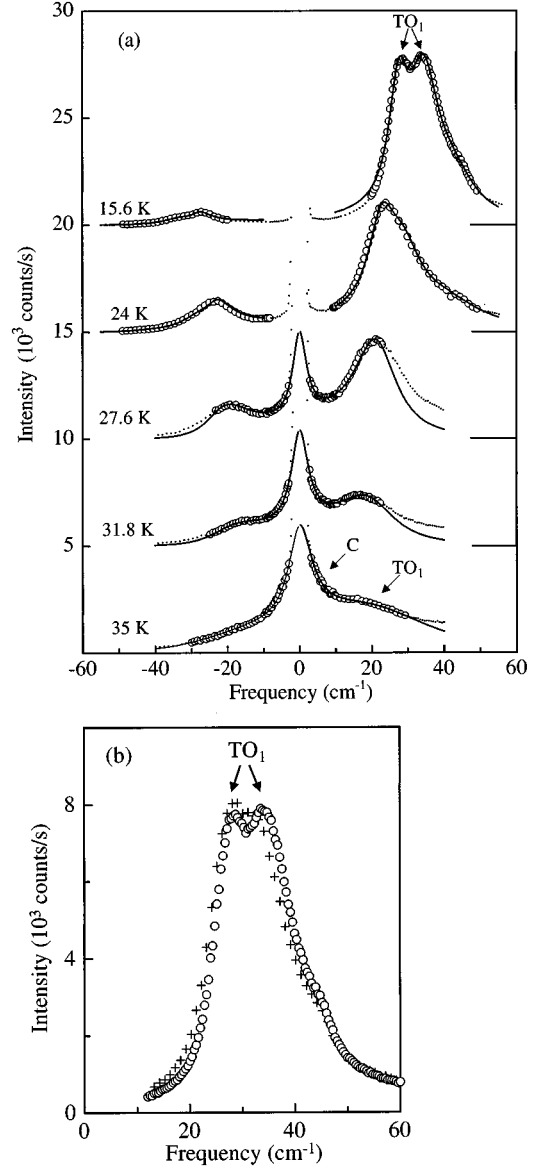


FIG. 1. (a) Low-frequency Raman spectra of KTN obtained in zero-field-cooling conditions at different temperatures (C denotes central peak). Solid curves: fitting to a relaxor-oscillator coupling model ($27 \text{ K} < T < 35 \text{ K}$) and to an uncoupled oscillators model ($T < 27 \text{ K}$). In the latter range additional TA structure at $\approx 45 \text{ cm}^{-1}$ has been taken into account by a harmonic oscillator. Fitted data are represented by open symbols. (b) Low-frequency Raman spectrum of KTN at 17 K after field cooling at 2 kV/cm (crosses) and zero-field cooling (open circles).

ational mode and soft mode is taken into account; (ii) a low temperature one, where coupling may be neglected.

In the first region, ranging approximately from 35 to 27 K, the Stokes and anti-Stokes portions of the spectra were found to fit a model cross section $S(\omega) = f(\omega) \text{Im}T(\omega)$, where $f(\omega)$ is the appropriate thermal factor and $T(\omega)$ is an oscillator-relaxor response function:¹⁴

$$T(\omega) = \left[\omega_0^2 - \omega^2 - 2i\omega\Gamma_0 - \frac{i\omega\tau\delta^2}{1 - i\omega\tau} \right]^{-1}. \quad (1)$$

In Eq. (1) ω_0 is the “naked” TO_1 frequency, Γ_0 is the

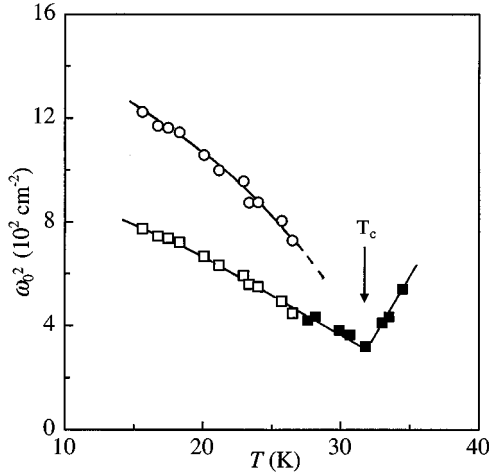


FIG. 2. Soft-mode squared frequency vs temperature in KTN. Data derived from spectral fitting to models of (i) relaxor-oscillator coupling, black symbols and (ii) uncoupled oscillators, open symbols. Lines are a guide to the eye.

phonon damping rate, τ is the relaxation time, and δ is the coupling parameter of the two modes. The quality of fitting is illustrated in the same figure 1(a) by the three lower curves: notice that below T_c , where the TO_1 line begins to split, only its low-frequency component is reproduced by this single-oscillator model. The best-fit ω_0 should actually represent such component. The values of ω_0 are plotted as black dots in Fig. 2; they are seen to soften and subsequently to harden, reaching a minimum at 32 K, in excellent agreement with the onset of birefringence. Best-fit values of the other parameters at different temperatures are listed in Table I: they compare favorably with previous findings on $\text{KTa}_{0.968}\text{Nb}_{0.032}\text{O}_3$.¹⁴

In the second region ($T < 27$ K) the overlap of TO_1 components, corresponding to phonons of different symmetry, was easily fitted by the response of two independent oscillators, as shown in the two upper spectra of Fig. 1(a). Frequencies obtained by this model are seen to harden on decreasing temperature, with a final splitting of about 6.5 cm^{-1} at 15 K (see open symbols in Fig. 2).

The validity of the whole analysis is confirmed by (i) the continuity in the frequency values obtained by the two different models and (ii) the agreement of $\omega_0(T_c)$, extrapolated from low-temperature data, with the directly fitted value.

One should note from the above data, the critical behavior of the TO_1 frequency, the line splitting, and the scarce sen-

TABLE I. Values of the parameters fitting the low-frequency spectrum of KTN in the relaxor-oscillator coupling model (Eq. 1).

T (K)	ω_0 (cm^{-1})	Γ_0 (cm^{-1})	τ^{-1} (cm^{-1})	δ (cm^{-1})
35	27.2	43.4	5.45	14.9
34.5	24.8	38.3	4.70	14.2
33.5	22.1	31.9	4.21	12.5
31.8	18.3	18.8	4.07	11.4
30.7	19.1	19.5	3.76	12.8
30	19.8	19	2.96	12.5
28.2	20.9	14.9	2.88	10.3
27.6	20.6	14	2.87	9.7

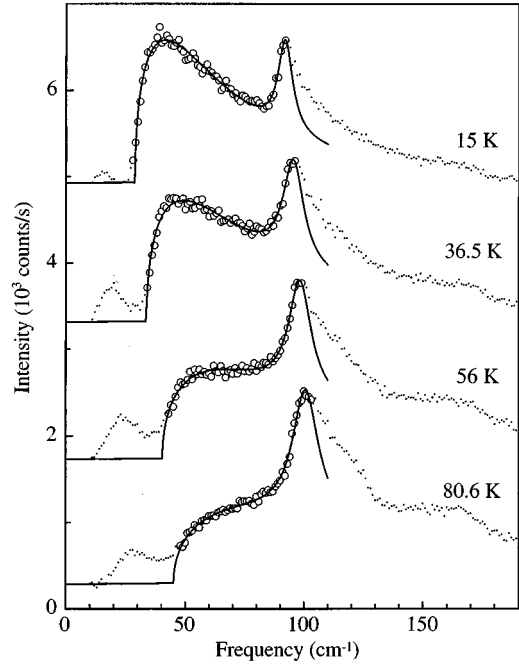


FIG. 3. Low-frequency Raman spectra of KLT obtained in zero-field cooling at different temperatures. Solid curves: fitting to a model of inhomogeneously broadened TO_1 [Eq. (4)] plus a Lorentzian 2TA line at $\approx 100 \text{ cm}^{-1}$. Fitted data are denoted by open symbols.

sitivity of the low temperature spectrum to cooling conditions (ZFC vs FC). These points, together with the abrupt enhancement of the TO_1 line strength below T_c , clearly suggest that long-range order is achieved already in the spontaneous case. Line splitting, previously resolved only in samples containing more than 3% mol Nb,³⁴ is a special indicator of this situation. If dipolar disorder (microclusters) were important in the low temperature phase, splitting should be blurred by anisotropy effects, as indeed happens in KLT at low concentrations.²⁷

As to incomplete softening, it is predicted by general theories of structural phase transitions, taking into account the soft mode-relaxational mode coupling.³⁵

KLT. The low-frequency spectrum and its temperature evolution in different poling conditions are quite distinct from the KTN case. The broad TO_1 line, observed in ZFC, shows moderate dependence on temperature, with no critical features as regards intensity or linewidth on going through T_f (Fig. 3). We note the large asymmetric broadening of this spectrum, extending approximately from 30 to 170 cm^{-1} , well beyond the 2TA component even at the lowest temperatures. This cannot be justified with a superposition of mixed-frequency modes, arising from anisotropy, as proposed by Prater *et al.* for higher dopant concentration.²⁷ In fact, the difference between ordinary and extraordinary TO_1 frequencies is known for our sample²⁸ to be less than $\sim 10 \text{ cm}^{-1}$, which is too small.

Broadening should then be ascribed to scattering from phonons of the whole TO_1 branch, due to wave-vector non-conservation in the presence of short-range polar order. Actually dispersion data on pure KTaO_3 (Ref. 36) show for this branch an upper limit at $\sim 170 \text{ cm}^{-1}$, matching the high-frequency cutoff of the Raman line.

One can attempt to relate the observed line shape with the presence of polar microdistortions, starting from a general expression of the cross-section, as follows:

$$S(\mathbf{q}, \omega) \div \langle \delta\chi(\mathbf{r}, t) \delta\chi(0, 0) \rangle_{\mathbf{q}, \omega} \div [\langle P(\mathbf{r}) P(0) \rangle \times \langle U(\mathbf{r}, t) U(0, 0) \rangle]_{\mathbf{q}, \omega}. \quad (2)$$

Here the correlation function for susceptibility is factorized in two parts, representing (i) correlation of the static order parameter $P(\mathbf{r})$, i.e., local polarization and (ii) dynamic correlation of independent phonon oscillators, $U(\mathbf{r}, t)$. Equation (2) obviously implies a linear coupling of $\delta\chi$ to local deformation, with a coupling coefficient independent of \mathbf{q} .

With the help of the convolution theorem, ignoring phonon damping and assuming isotropic dispersion, Eq. (2) becomes

$$S(\omega) \div \frac{f(\omega)}{\omega} D(\omega) G(q_\omega), \quad (3)$$

where $f(\omega)$ is the Bose factor, $G(q_\omega) = \langle P(r) P(0) \rangle_{q_\omega}$, and $D(\omega)$ is the phonon density of states. At this point, explicit modeling of the cross section depends on the particular expression of $G(q_\omega)$. In analogy with the case of spin-glass systems,³⁷ we assume here a phenomenological form $\langle P(r) P(0) \rangle \div \exp(-r/\xi)$, as a model of dipolar correlation with a characteristic length ξ .

With the above positions and assuming for dispersion the usual form $\omega_q^2 = \omega_0^2 + v^2 q^2$, Eq. (3) is finally transformed to

$$S(\omega) \div f(\omega) \frac{v}{\xi} \frac{\sqrt{\omega^2 - \omega_0^2}}{\left(\omega^2 - \omega_0^2 + \frac{v^2}{\xi^2}\right)^2}. \quad (4)$$

Equation (4) represents the cross section used to fit the experimental TO_1 spectra. Actually, a Lorentzian term was added to this, in order to account for the low-frequency side of the nearby 2TA band. Data on the tail beyond this band were not fitted for two reasons: (i) the assumed density of states is not expected to hold in the zone boundary limit; (ii) the q dependence of the coupling coefficient is not considered in our simple model. Best fit of representative spectra obtained in the range 15–80 K in ZFC conditions is illustrated in the same Fig. 3.

The relevant parameters in this analysis are the frequency ω_0 and the ratio v/ξ . Temperature evolution of these quantities, taken from a complete series of spectra, is shown in Fig. 4. The frequency exhibits a slight, noncritical softening. The other parameter undergoes a sizeable decrease (by a factor ~ 3). Notice that the treatment of Eq. (4) does not assume any special relationship between v/ξ and ω_0 : the trend observed in Fig. 4 confirms that these parameters are quite independent, at variance with the assumption of other models of light scattering near a phase transition.³⁸ This is a direct indication that the polar pattern is not controlled by soft-mode dynamics.

Knowledge of v/ξ allows us to evaluate the correlation length, using for v a value of $\sim 10^{-5}$, which one estimates from existing dispersion data for the TO_1 branch at low T (Ref. 36) [the same figure was employed by Uwe *et al.* in their study on nominally pure or very diluted KTaO_3 (Ref.

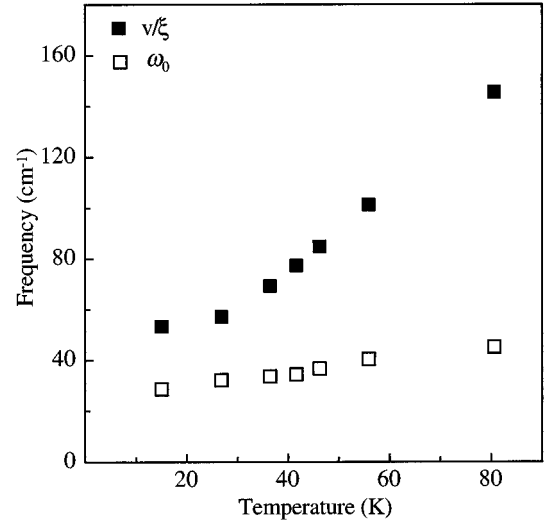


FIG. 4. Temperature dependence of best-fit TO_1 parameters in KLT.

29)]. The values obtained for ξ in this assumption are plotted in Fig. 5, showing that the ordering length is limited to the nanometric scale over the entire range, with no sign of critical increase below T_f .

One should also observe that the present analysis is not immediately comparable with that of Uwe *et al.*,²⁹ concerning KTaO_3 with $\sim 0.9\%$ mol Nb. In that case, ξ was defined as the range of disturbance of diluted point defects, in an otherwise homogeneous matrix. In our case, it represents the ordering scale of a polarized medium, which possibly accounts for an interaction among defects. The present results confirm most directly that KLT behaves as an assembly of frozen dipolar regions, in agreement with recent findings from second-harmonic generation in the same KLT sample.²⁴

We also attempted to fit the same spectra by means of an alternative version of Eq. (4), which one obtains in the hypothesis of an Ornstein-Zernike (OZ) correlation function

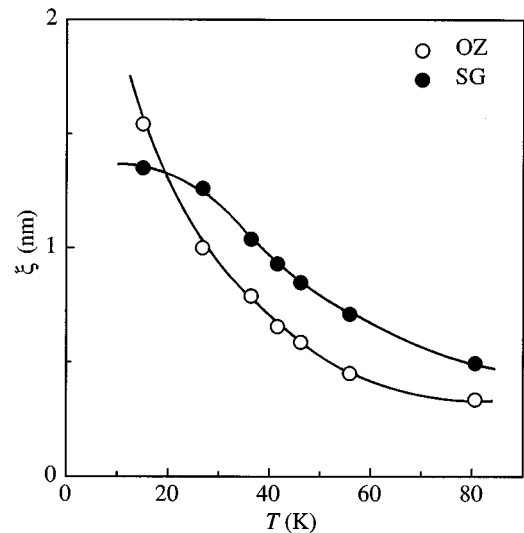


FIG. 5. Temperature dependence of the polar correlation length ξ in KLT. Black symbols: as derived from the data of Fig. 4, spin-glass correlation, SG. Open symbols: from an Ornstein-Zernike correlation model. Lines are a guide to the eye.

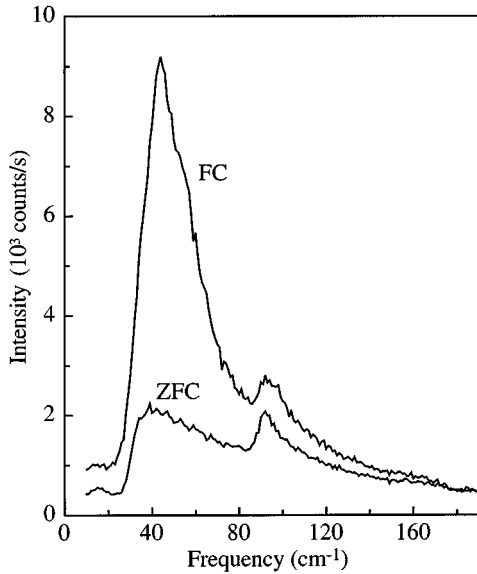


FIG. 6. TO_1 spectrum of KLT at 15 K after zero-field cooling or field cooling (2 kV/cm).

$\langle P(r)P(0) \rangle \div r^{-1} \exp(-r/\xi)$. In Fig. 5, the results are compared with those of the spin glass model: the apparent divergence of correlation for $T \rightarrow 0$ K, given by the OZ model, is unphysical, since the freezing temperature is anyhow finite.

As shown in previous work,³⁹ the spectra obtained in field-cooling conditions have a different evolution. In the poled sample, the TO_1 line narrows below the freezing temperature, showing a more symmetric profile and a strong intensity increase. As an example, Fig. 6 compares two spectra in different poling conditions at low temperature. Such behaviour implies a marked enhancement of polar order, induced by the field. Here the basic assumptions of our model should fail, because natural broadening is no more negligible and an isotropic correlation function is no longer suited. This explains why the fitting of FC spectra with the same model was unsuccessful.

B. Hard-phonon spectra

High-frequency Raman spectra were taken in parallel with the soft-phonon spectra. Intensity data for the narrow and asymmetric TO_2 line were obtained by direct integration. The TO_4 line is broader and more symmetrical and was fitted by a Lorentzian in all cases, treating the overlap with the second-order TO_4+TA structure with an additional Lorentzian term (see, for instance, Fig. 7). Intensity and linewidth were derived with the help of this analysis. We restrict in the following to a few aspects of hard-phonon behavior, which allow us to stress a persisting difference between KTN and KLT.

Figure 8 summarizes the results concerning the strength of the polar-phonon lines TO_2 and TO_4 . In the case of KTN, detectable growth begins only a few degrees above T_c and the line strength rapidly increases below that point, even in the absence of poling. A small and reproducible maximum develops above the transition in TO_4 and probably is present also in TO_2 ; this precursor effect is already known for other perovskites with structural phase transitions.³³ The behavior in KLT is different, inasmuch as the two lines are detectable well above the freezing temperature. Most important, their

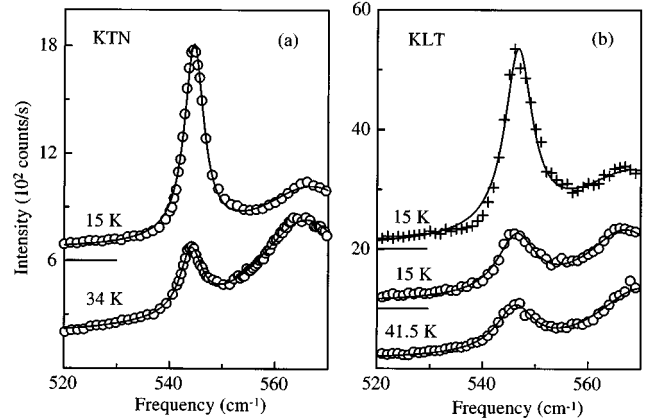


FIG. 7. TO_4 spectra of KTN (a) and KLT (b) at different temperatures. Circles and crosses refer to ZFC and FC conditions, respectively. Solid curves describe Lorentzian fitting (see text).

strength is substantially constant over the entire temperature range in zero field, but is strongly enhanced below T_f when a field is applied (a similar trend was previously reported for the TO_1 mode³⁹). Notice that the increments of TO intensities in field-cooled KLT are probably underestimated near T_f , as a result of photoinduced depolarization as discussed in Sec. II. At the lowest temperatures, where this artifact is uneffective, the intensities should give a correct indication of the poling attainable in the external field.

Information can also be drawn from the behavior of the TO_4 linewidth, whose temperature dependence is illustrated in Fig. 9. Clearly, a marked narrowing takes place in KTN on lowering the temperature towards T_c ; at this point the trend is interrupted and no further variation occurs on cooling. In the same zero-field conditions, the width is nearly constant in KLT over the entire range; partial narrowing is introduced below T_f if poling is present.

This line-shape behavior might be ascribed, by analogy with the arguments adopted for TO_1 in KLT, to the combined effects of mode dispersion and short-range order. On these

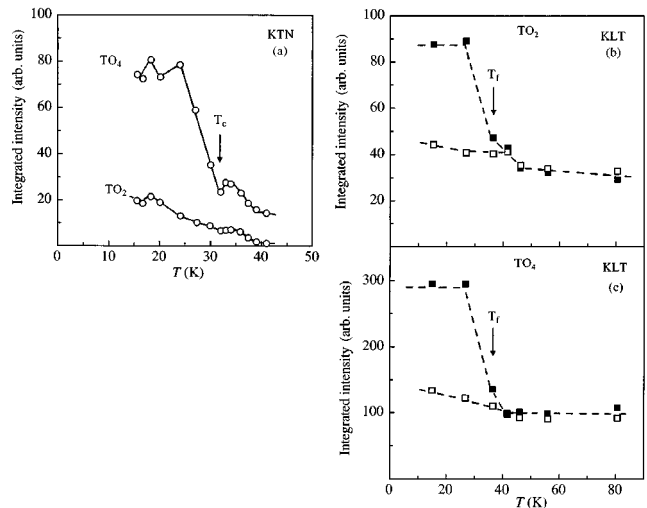


FIG. 8. Temperature dependence of integrated intensities for the polar-phonon lines: (a) KTN; (b), (c) KLT. Open and black symbols refer to ZFC and FC experiments, respectively. Lines are a guide to the eye.

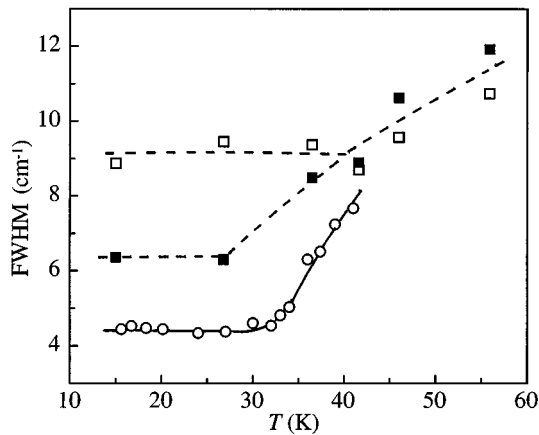


FIG. 9. Full width at half maximum of the TO_4 line of KTN (circles) and KLT (squares). Open and black symbols refer to ZFC and FC experiments, respectively. Lines are a guide to the eye.

grounds the rapid decrease and the subsequent slowdown indicate for KTN a fast evolution of precursor phenomena, ending in a low temperature phase where order is complete. A similar behavior, reported for the hard-phonon E_g line of $KMnF_3$ and $RbCaF_3$, has been explained in the same way.³³ The results for KLT represent the alternative case of frozen short-range order, which can be modified by a poling field.

In recent work,¹⁸ a quantitative analysis of the TO_2 spectrum has been attempted, using a model of inhomogeneous broadening as an alternative to a Fano coupling mechanism.⁴⁰ The results are claimed to support the idea of a persistent polar disorder, as a common characteristic of KLT and KTN in a wide range of concentrations. Data on polar correlation, derived in this frame, are in fair agreement with those obtained by different means for KLT;²⁴ however, they do not seem to warrant a sure indication for what concerns KTN, far below the transition temperature. We remark anyhow that similar effects of polar disorder should show up *a fortiori* in the soft mode, owing to its larger dispersion. This

is clearly contradicted by the absence of asymmetric broadening in the TO_1 spectrum of KTN, commented before.

IV. CONCLUSIONS

The analysis of TO_1 spectra in KLT with 1.6% mol Li reveals broadening effects, which are related to a very short scale of polar order below T_f . A spin-glass correlation function is found to be suitable in describing the pattern of *spontaneous* polarization. The correlation length is limited to a few nanometers and is unrelated to the TO_1 frequency. This confirms that the transition is controlled by Li-Li interactions rather than soft-mode dynamics. The strength and width of the hard-phonon lines, showing little evolution in the spontaneous case but strong dependence on poling, are also consistent with the dipole-glass picture.

In KTN with 2.4% mol Nb the spectral shape and the frequency behavior of TO_1 are consistently described by a coupling of the soft mode to relaxational motions, which rapidly ceases to be effective below T_c . No evidence is present in TO_1 spectrum that might indicate the persistence of microclustering at low temperature: on the contrary, the occurrence of definite splitting and the absence of field-cooling effects in the line strength are elements in favor of long-range order. The evolution of the TO_4 line gives further support to this picture. One should conclude for a proper cooperative transition, in which clustering does not prevent the attainment of an ordered structure, even in this limit of concentration (though, of course, it may influence the transition kinetics around T_c).

The extent of the observed pretransitional effects is related to the different role of the impurities. In KLT, the hopping frequency of Li ions is much lower than the TO mode frequencies,³¹ so that quasistatic distortions of the host matrix are induced by off-center displacements above T_f . In KTN first-order Raman scattering is activated a few degrees above T_c , indicating that order parameter fluctuations induced by the impurity occur on a temporal scale higher than that of TO vibrations. This behavior is inherent to the dynamics of a displacive system near its critical point.³³

¹U. T. Höchli, K. Knorr, and A. Loidl, *Adv. Phys.* **39**, 405 (1990).

²B. E. Vugmeister and M. D. Glinchuk, *Rev. Mod. Phys.* **62**, 993 (1990).

³W. Kleemann, *Int. J. Mod. Phys. B* **7**, 2469 (1993).

⁴G. E. Kugel, M. D. Fontana, and W. Kress, *Phys. Rev. B* **35**, 813 (1987).

⁵L. A. Boatner, U. T. Höchli, and H. Weibel, *Helv. Phys. Acta* **50**, 620 (1977).

⁶G. E. Kugel, H. Vogt, W. Kress, and D. Rytz, *Phys. Rev. B* **30**, 985 (1984); G. E. Kugel, M. D. Fontana, H. Mesli, and D. Rytz, *Jpn. J. Appl. Phys. Suppl.* **24**, 226 (1985).

⁷S. Rod, F. Borsa, and J. J. van der Klink, *Phys. Rev. B* **38**, 2267 (1988).

⁸J. J. van der Klink, S. Rod, and A. Chatelain, *Phys. Rev. B* **33**, 2084 (1986).

⁹K. B. Lyons, P. A. Fleury, and D. Rytz, *Phys. Rev. Lett.* **57**, 2207 (1986).

¹⁰M. D. Fontana, M. Maglione, and U. T. Höchli, *J. Phys. Condens. Matter* **5**, 1895 (1993).

¹¹W. Kleemann, F. J. Schäfer, and D. Rytz, *Phys. Rev. Lett.* **54**, 2038 (1985).

¹²G. A. Samara, *Phys. Rev. Lett.* **53**, 298 (1984).

¹³P. M. Gehring, H. Chou, S. M. Shapiro, J. A. Hriljac, D. H. Chen, J. Toulouse, D. Rytz, and L. A. Boatner, *Phys. Rev. B* **46**, 5116 (1992).

¹⁴E. Lee, L. L. Chase, and L. A. Boatner, *Phys. Rev. B* **31**, 1438 (1985).

¹⁵M. D. Fontana, E. Bouziane, and G. E. Kugel, *J. Phys. Condens. Matter* **2**, 8681 (1990).

¹⁶H. Chou, S. M. Shapiro, K. B. Lyons, J. Kjemis, and D. Rytz, *Phys. Rev. B* **41**, 7231 (1990).

¹⁷J. Toulouse, P. DiAntonio, B. E. Vugmeister, X. M. Wang, and L. A. Knauss, *Phys. Rev. Lett.* **68**, 232 (1992).

¹⁸P. DiAntonio, B. E. Vugmeister, J. Toulouse, and L. A. Boatner, *Phys. Rev. B* **47**, 5629 (1993).

- ¹⁹J. J. van der Klink and F. Borsa, Phys. Rev. B **30**, 52 (1984).
- ²⁰M. G. Stachiotti and R. L. Migoni, J. Phys. Condens. Matter **2**, 4341 (1990).
- ²¹H. Vollmayr, R. Kree, and A. Zippelius, Phys. Rev. B **44**, 12 238 (1991).
- ²²M. G. Stachiotti, R. L. Migoni, H-M Christen, J. Kohanoff, and U. T. Höchli, J. Phys. Condens. Matter **6**, 4297 (1994).
- ²³U. T. Höchli and M. Maglione, J. Phys. Condens. Matter **1**, 2241 (1989); F. Wickenhofer, W. Kleemann, and D. Rytz, Ferroelectrics **124**, 237 (1991).
- ²⁴G. A. Azzini, G. P. Banfi, E. Giulotto, and U. T. Höchli, Phys. Rev. B **43**, 7473 (1991); G. P. Banfi, P. Calvi, and E. Giulotto, Phys. Rev. B **51**, 6231 (1995).
- ²⁵P. Doussineau, C. Frenois, A. Levelut, and S. Ziolkiewicz, J. Phys. Condens. Matter **3**, 8369 (1991).
- ²⁶D. Sommer, W. Kleemann, M. Lehndorff, and K. Dransfeld, Solid State Commun. **72**, 731 (1989).
- ²⁷R. L. Prater, L. L. Chase, and L. A. Boatner, Phys. Rev. B **23**, 5904 (1981).
- ²⁸G. P. Banfi, P. Camagni, E. Giulotto, G. Samoggia, and U. T. Höchli, Ferroelectrics **124**, 133 (1991).
- ²⁹H. Uwe, K. B. Lyons, H. L. Carter, and P. A. Fleury, Phys. Rev. B **33**, 6436 (1986).
- ³⁰G. P. Banfi, P. Calvi, P. Camagni, E. Giulotto, and G. Samoggia, Ferroelectrics **106**, 143 (1990).
- ³¹J. J. van der Klink, D. Rytz, F. Borsa, and U. T. Höchli, Phys. Rev. B **27**, 89 (1983).
- ³²R. S. Klein, G. E. Kugel, M. D. Glinchuk, R. O. Kuzian, and I. V. Kondakova, Phys. Rev. B **50**, 9721 (1994).
- ³³A. D. Bruce, W. Taylor, and A. F. Murray, J. Phys. C **13**, 483 (1980).
- ³⁴R. L. Prater, L. L. Chase, and L. A. Boatner, Phys. Rev. B **23**, 221 (1981).
- ³⁵V. L. Ginzburg, A. P. Levanyuk, and A. A. Sobyenin, Phys. Rep. **57**, 151 (1980).
- ³⁶C. H. Perry, R. Currat, H. Buhay, R. M. Migoni, W. G. Stirling, and J. D. Axe, Phys. Rev. B **39**, 8666 (1989).
- ³⁷K. Binder and A. P. Young, Rev. Mod. Phys. **58**, 801 (1986).
- ³⁸A. P. Levanyuk and A. S. Sigov, *Defects and Structural Phase Transitions* (Gordon and Breach, New York, 1988).
- ³⁹G. P. Banfi, P. Calvi, P. Camagni, E. Giulotto, and G. Samoggia, *Proceedings of the International Conference on Defects in Insulating Materials*, Nordkirchen, Germany, 1992 (World Scientific, Singapore, 1993), Vol. 1, p. 660.
- ⁴⁰Y. Yacoby, Z. Phys. B **31**, 275 (1978).